Lab on a Chip

Accepted Manuscript

ROYAL SOCIETY OF CHEMISTRY

www.rsc.org/loc

Lab on a Chip

RSCPublishing

TECHNICAL INNOVATION

Dual-mode hydrodynamic railing and arraying of microparticles for multi-stage signal detection in continuous flow biochemical microprocessors†

Cite this: DOI: 10.1039/x0xx00000x

Ryan D. Sochol,*[ad] Daniel Corbett,[bd] Sarah Hesse,[cd] William E.R. Krieger,[ad] Ki Tae Wolf,[ad] Minkyu Kim,[ad] Kosuke Iwai,[ad] Song Li,[b] Luke P. Lee[bd] and Liwei Lin[ad]

Received 00th January 2014,
Accepted 00th January 2014

DOI: 10.1039/x0xx00000x

www.rsc.org/

Continuous flow particulate-based microfluidic processors are in critical demand for emerging applications in chemistry and biology, such as point-of-care molecular diagnostics. Challenges remain, however, for accomplishing biochemical assays in which microparticle immobilization is desired or required during intermediate stages of fluidic reaction processes. Here we present a dual-mode microfluidic reactor that functions autonomously under continuous flow conditions to: (*i*) execute multi-stage particulate-based fluidic mixing routines, and (*ii*) array select numbers of microparticles during each reaction stage (*e.g.*, for optical detection). We employ this methodology to detect the inflammatory cytokine, interferon-gamma (IFN-γ), *via* a six-stage aptamer-based sandwich assay.

Introduction

Particulate-based microfluidic technologies offer significant scaling-induced advantages for biochemical applications, such as pharmacological screening, molecular detection, and quantitative cellular diagnostics.[1, 2] In particular, bead-based microfluidic systems benefit from high surface-to-volume ratios, rapid reaction kinetics, low reagent volumes, and the ability to functionalize microbeads with surface modifications, including molecular probes capable of detecting a wide range of chemicals and biomolecules.[1-5] Consequently, researchers have focused on developing bead-based microfluidic platforms for chemical and biological assays (*e.g.*, immunoassays); however, challenges stemming from the serial fluidic loading requirements associated with such assays have limited the versatility of current systems.[5-7] Specifically, biochemical assays primarily utilize multi-stage fluidic processes in which discrete reagents and/or washes are sequentially loaded, resulting in microfluidic systems that typically require external observation and/or regulation during device operation.[8-10] This issue presents additional challenges for fluidic assays that necessitate microbead immobilization (*e.g.*, for visualization and/or fluorescence signal detection) during intermediate steps over the course of such multi-stage processes. Thus, methods to fully automate multi-stage fluidic mixing procedures, while enabling targeted microparticle immobilization, could vastly improve the efficacy of microfluidic biochemical reactors.

Recently, researchers have focused on developing microfluidic techniques to passively transport microparticles into discrete, parallel flow streams under continuous and constant input flow conditions.[11-16] Previously, we presented a microfluidic system that utilized microposts arrayed at an angle with respect to the direction of fluid flow to hydrodynamically guide suspended microbeads and living cells into distinct, adjacent flow streams.[16] Although we employed this technique to passively accomplish molecular synthesis processes with up to 18 fluidic stages using microbead substrates, immobilization of microparticles was not possible until completion of the full reaction process.[16] This is a significant limitation for biochemical assays such as aptamer beacon-based assays that require positive and negative controls of fluorescence intensities prior to reaction completion.[3] To overcome this drawback, here we present a dual-mode continuous flow "rail-trap-and-rail" methodology for autonomously executing multi-stage particulate-based microfluidic mixing reactions, while enabling the immobilization of select numbers of microparticles in designated array positions corresponding to each fluidic reaction step (Fig. 1). We utilize this technique to passively accomplish a six-stage aptamer beacon-based sandwich assay to detect the inflammatory cytokine, interferon-gamma (IFN-γ).

[a] Department of Mechanical Engineering, University of California, Berkeley, USA. E-mail: rsochol@gmail.com; Tel: +1 410 935 8971
[b] Department of Bioengineering, University of California, Berkeley, USA
[c] Department of Chemistry, University of California, Berkeley, USA
[d] Berkeley Sensor and Actuator Center (BSAC), Biomolecular Nanotechnology Center (BNC), University of California, Berkeley, USA
† Electronic Supplementary Information (ESI) available: COMSOL Multiphysics simulations, microdevice fabrication, illustrations and equations for device performance, results for signal intensity with time, and movies of microbead dynamics. See DOI: 10.1039/b000000x/

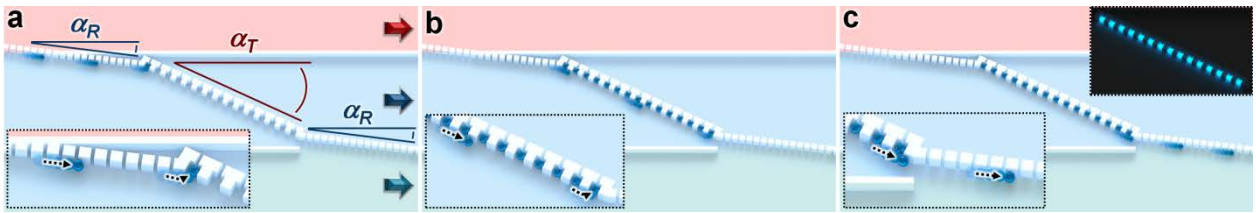

Fig. 1 Illustrations of the continuous flow microfluidic "rail-trap-and-rail" concept. (a) Square-shaped microposts arrayed at a railing angle (α_R; with respect to the flow direction) serve as a railing system for passively transporting suspended microparticles into distinct, parallel flow streams and then into the trapping area. (b) Microparticle trapping sites arrayed at a trapping angle (α_T) promote the immobilization of select numbers of suspended microparticles into designated array positions. (c) After completion of the arraying process, immobilized microparticles can be visualized using fluorescence microscopy (*inset*). Subsequently loaded microparticles are guided past the arrayed particles and into adjacent flow streams. This process can be repeated as desired. Illustrations are not to scale.

Materials and Methods

Microfluidic "rail-trap-and-rail" concept

Figure 1 includes conceptual illustrations of the dual-mode hydrodynamic methodology, which utilizes square-shaped microposts and microparticle trapping sites that are arrayed at a railing angle (α_R) or a larger trapping angle (α_T), to prevent or promote particle immobilization, respectively (ESI Fig. 1). Under continuous input flow conditions, the arrayed microposts (of approximately the same size as the target microparticles) passively guide suspended microparticles into discrete, parallel flow streams (without altering the direction of the inputted fluid flow) and toward the trapping area (Fig. 1a). The suspended microparticles passively immobilize in the designated trapping sites, which diverts fluid flow from the occupied traps to the remaining vacant trapping positions. This process facilitates the transport and immobilization of subsequent microparticles into the remaining vacant trapping sites until the trapping area is filled (Fig. 1b). Thereafter, additional suspended microparticles are guided past the previously immobilized particles and into the next micropost array railing area to be transported into a subsequent adjacent fluidic stream (Fig. 1c). This process can be repeated continuously as desired with additional fluidic reagents and/or washes loaded in parallel to customize the microfluidic rail-trap-and-rail system for diverse multi-stage fluidic processes that demand select microparticle immobilization corresponding to intermediate reaction steps.

Continuous flow detection of interferon-gamma (IFN-γ) *via* an aptamer beacon-based sandwich assay

To detect the inflammatory cytokine, IFN-γ, we applied the microfluidic rail-trap-and-rail methodology to execute a six-step aptamer beacon-based sandwich assay under continuous input flow conditions. Figure 2 includes conceptual illustrations of the system architecture and reaction process. The aptamer beacon used in this study was designed previously by Tuleuova *et al.*, and consists of two complementary single-stranded DNA sequences: a fluorescent aptamer (FA), and a quencher (Q) (ESI Table 1).[3] Six suspensions/solutions were continuously loaded in parallel: (*i*) a suspension of microbeads functionalized with an avidin-based biological linker, (*ii*) a solution of biotinylated FAs, (*iii*) a wash solution of phosphate-buffered saline (PBS), (*iv*) a solution of Qs, (*v*) a second solution of PBS, and (*vi*) a solution of IFN-γ (Fig. 2a). Initially, the functionalized beads are transported into the FA solution, which promotes the binding of biotinylated FAs to the micro-

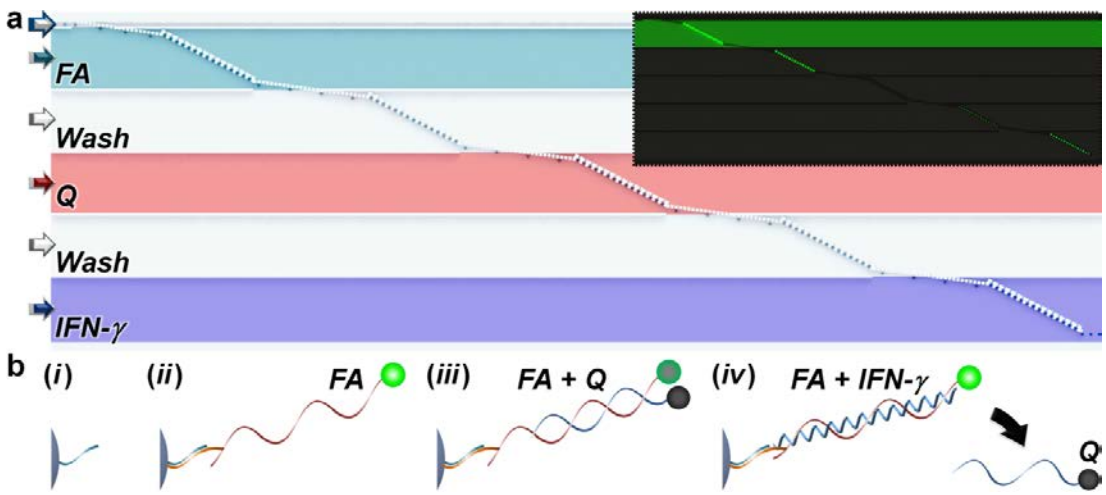

Fig. 2 Illustrations of the continuous flow bead-based microfluidic reactor for detecting interferon-gamma (IFN-γ) *via* an aptamer-based sandwich assay. (a) The microfluidic system architecture (not to scale). Six discrete, homogenous fluidic suspensions, reagents, and washes are continuously loaded into the system in parallel. The microbeads are passively transported into the discrete flow streams with select bead trapping. Fluorescence intensities of arrayed microbeads corresponding to each fluidic stage can be detected (*inset*). (b) The aptamer-based sandwich assay process. (*i*) Microbeads are functionalized with an avidin-based biological linker. (*ii*) Biotinylated Fluorescent Aptamers (FAs) are conjugated to the microbeads *via* biotin-avidin binding interactions, resulting in fluorescence. (*iii*) Complementary Quenchers (Qs) bind to the FAs, which restrict fluorescence. (*iv*) IFN-γ displaces the Qs and binds to the FAs, increasing the fluorescence signal.

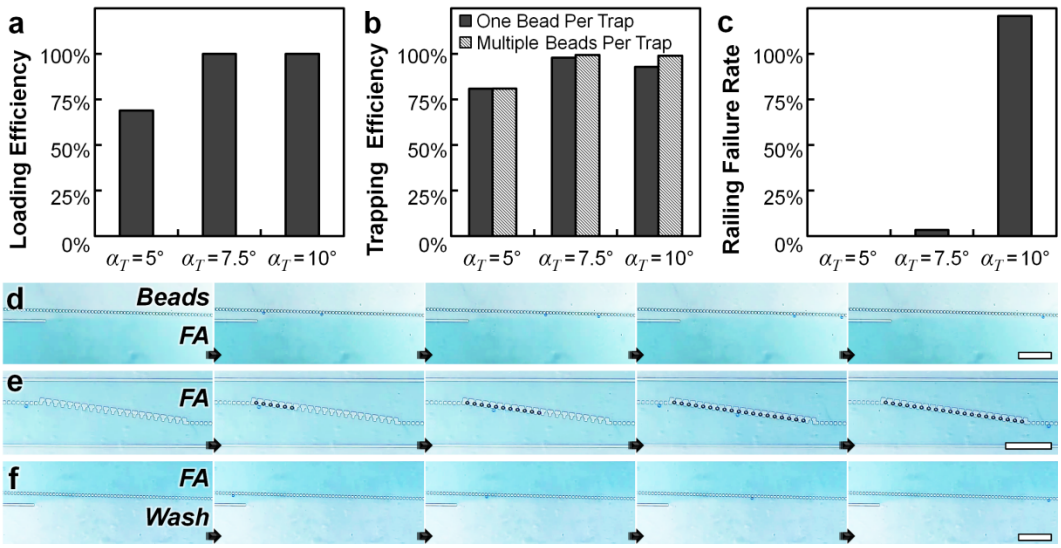

Fig. 3 Experimental results for microbead dynamics. (a-c) Quantified results for: (a) Loading Efficiency, (b) Trapping Efficiency, and (c) Railing Failure Rate (ESI Eq. 1-3) *versus* varying α_T. (d-f) Sequential micrographs of microbeads (15 μm in diameter): (d) railing from the bead suspension into the FA solution, (e) arraying in the designated trapping sites, and (f) railing from the FA solution to the wash solution. Scale Bars = 200 μm; α_R = 1°; α_T = 7.5°. ESI Movie 1 includes video of this process.

bead substrate *via* biotin-avidin interactions (Fig. 2b – *i-ii*). This results in detectable fluorescence on the surface of the microbeads (Fig. 2a – *inset*). After passing through the PBS wash solution, mixing reactions with the Q solution promote binding of the Qs to complementary FAs, thereby restricting the fluorescence intensity (Fig. 2a; Fig. 2b – *iii*). Following a second wash, additional microbeads are guided into the IFN-γ solution to promote the displacement of Qs by IFN-γ, which enhances the fluorescence response (Fig. 2a; Fig. 2b – *iv*). The fluorescence signals of arrayed microbeads can be detected for each fluidic stage of the assay process (Fig. 2a – *inset*).

Experimental

Microdevices were fabricated *via* a previously reported one-mask soft lithography process (ESI Fig. 2).[16, 17] The devices were designed for 15 μm-in-diameter streptavidin-coated polystyrene microbeads (#SVP-150-4, Spherotech, Inc., Lake Forest, IL). The beads were functionalized with an additional biotin-avidin pair to enhance the fluorescence intensities.[16] Due to the polydispersity of the microbeads, the devices included microchannel heights of 18 μm, with 5 μm gaps between the microposts (15×15 μm^2) and traps. The channel lengths for microfluidic mixing were designed as described previously.[16] Fabrication results for microfluidic rail-trap-and-rail systems with α_R = 1° and α_T = 7.5° are shown in ESI Fig. 3.

The microdevices were pre-treated with Tween 20 (10% in PBS, Fisher Scientific, Pittsburgh, PA).[16] We used the Fluigent MAESFLO system to regulate the flow rates (approximately 3 μL/min) of the six input fluids: (*i*) microbead suspension (30 beads/μL), (*ii*) FA solution (100 μM), (*iii*) Q solution (100 μM), (*iv*) IFN-γ solution (10 μM; R&D Systems, Inc, Minneapolis, MN), and two PBS wash solutions (#14287072, Invitrogen Corp., Carlsbad, CA). The full bead-based experimental process was accomplished within 10 minutes. Fluorescence intensities of immobilized microbeads were quantified using ImageJ (NIH, Bethesda, MD). Experimental fluorescence results are presented in the text as mean ± s.e.m.

Results and discussion

Experimental characterization of the effects of the trapping angle (α_T) on "rail-trap-and-rail" performance

Experiments were performed using testing systems with α_T = 5°, 7.5°, and 10° (while α_R was held constant at 1°) in order to examine the effects of α_T on device performance. Previously reported equations for quantifying the efficiencies associated with microbead arraying[17] and railing[16] were used to characterize device performance (ESI Fig. 4; ESI Eq. 1-3). For the α_T = 5° testing systems, microbeads often bypassed the trapping areas without being arrayed during the loading process, with primarily non-sequential loading (ESI Movie 2). The Loading Efficiency (LE) for the α_T = 5° system was 69% (n = 210 beads) (Fig. 3a). In contrast, systems with α_T = 7.5° and 10° trapping areas both exhibited LEs of 100% (n = 195 beads and 124 beads, respectively) (Fig. 3a). Similar behaviour was observed for the Trapping Efficiency (TE) performance, with α_T = 5° systems resulting in equivalent one-bead-per-trap and multiple-beads-per-trap TEs of 81% (n = 149 beads) (Fig. 3b). The α_T = 7.5° system was found to produce the largest one-bead-per-trap TE of 98% (n = 190 beads). The TE for the α_T = 10° system decreased slightly to 93% (n = 190 beads), which was due to multiple beads arraying on top of previously immobilized microbeads (resulting in a multiple-beads-per-trap TE of 99%). Additionally, the higher α_T = 10° was found to adversely affect the railing performance, with a Railing Failure Rate (RFR) of 121% (n = 105 potential failure sites) (Fig. 3c; ESI Movie 3). This RFR was significantly larger than the RFRs for the α_T = 5° and 7.5° cases, which were 0% and 3% (n = 120 and 150 potential failure sites), respectively (Fig. 3c). Experimental results revealed that α_T = 7.5° yielded the best balance of performance for both operating modes (*i.e.*, particle railing and arraying) of the system (Figure 3 and ESI Movie 1).

Continuous flow bead-based microfluidic detection of IFN-γ

The microfluidic reactor for detecting IFN-γ included railing

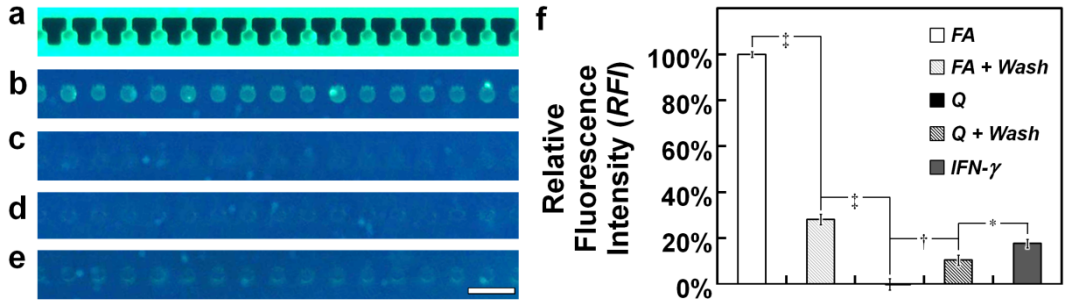

Fig. 4 Fluorescence results for the continuous flow microfluidic reactor for detecting IFN-γ. (a-e) Fluorescence micrographs of arrayed microbeads corresponding to the: (a) FA solution, (b) first PBS wash, (c) Q solution, (d) second PBS wash, and (e) IFN-γ solution. Scale Bars = 50 μm. (f) Average Relative Fluorescence Intensities corresponding to each reaction-step. Error Bars denote s.e.m.; *, †, and ‡ denote $p < 0.05$, $p < 0.005$, and $p < 0.0001$ statistically significant differences, respectively.

and trapping areas with α_R and α_T equal to 1° and 7.5°, respectively. Experimental device runs revealed that the microfluidic rail-trap-and-rail methodology successfully transported suspended microbeads into the distinct, parallel reagents and wash solutions, while trapping select numbers of microbeads in the array positions as designed (ESI Movie 1). For example, Figure 3d-f shows sequential micrographs of microbeads being passively: (d) transported from the bead suspension (*white*) to the FA solution (*cyan*), (e) arrayed in the FA solution trapping area, and then (c) guided from the FA solution to the PBS wash solution (*white*). After microbeads were immobilized in the designated trapping areas (Fig. 4a-e), Relative Fluorescence Intensities (RFIs) were quantified *via* ESI Eq. 4. The signal intensities exhibited minor variation with time (ESI Fig. 4). Each of the solutions produced statistically discernable RFIs (Fig. 4f). After mixing with the FA solution, the microbeads exhibited the highest average RFIs of 100%±1.3%. Mixing with the Q solution was found to significantly reduce the bead-based fluorescence response ($p < 0.0001$), revealing an average RFI of 0%±2.4%. After mixing with the IFN-γ, the average RFI increased significantly to 17.8%±1.8% ($p < 0.0001$), which was also discernible from the average RFI corresponding to the second PBS wash solution (10.6%±2.2%; $p < 0.05$) (Fig. 4f). These results demonstrate an aptamer-based detection sensitivity of 10 μM of IFN-γ for our assay reaction process.

Conclusions

Continuous flow methods for accomplishing multi-stage microfluidic mixing routines with controlled microparticle arraying are critical to the advancement of diverse chemical and biological applications. Here we presented and demonstrated a dual-mode hydrodynamic methodology by executing a six-stage aptamer beacon-based sandwich assay on microbead substrates under continuous flow conditions. Targeted microbead arraying enabled fluorescence quantification for every phase of the multi-stage process. Here, multi-step microfluidic reactions and analyses were performed to detect the cytokine, IFN-γ; however, microbeads can be functionalized with a variety of molecular probes, and thus, the presented technique could be adapted to accomplish a wide range of multi-step biochemical reaction processes. Additionally, the system in this work included microbeads and microfeatures of approximately the same size, which suggests that this technique could be scaled up or down to handle particles of various sizes. Thus, the presented rail-trap-and-rail methodology could greatly extend the efficacy of particulate-based microfluidic reactors.

Acknowledgements

The authors greatly appreciate the contributions of Mengqian Liu, Casey C. Glick, Nazly Pirmoradi, Jonathan Lei, Thomas Brubaker, Albert Lu, Adrienne T. Higa, Paul Lum, and the members of the Liwei Lin Laboratory, the Biologically-inspired Photonics-Optofluidic-Electronic Technology and Science (BioPOETS) group, the Song Li Laboratory, and the Micro Mechanical Methods for Biology (M^3B) Laboratory Program.

References

1 W. H. Tan and S. Takeuchi, *Proceedings of the National Academy of Sciences of the United States of America*, 2007, **104**, 1146-1151.
2 E. Verpoorte, *Lab on a Chip*, 2003, **3**, 60N-68N.
3 N. Tuleuova, C. N. Jones, J. Yan, E. Ramanculov, Y. Yokobayashi and A. Revzin, *Analytical Chemistry*, 2010, **82**, 1851-1857.
4 Y. Liu, T. Kwa and A. Revzin, *Biomaterials*, 2012, **33**, 7347-7355.
5 M. Tarn, M. Lopez-Martinez and N. Pamme, *Analytical and Bioanalytical Chemistry*, 2013, 1-23.
6 J. K. K. Ng and W. T. Liu, *Analytical and Bioanalytical Chemistry*, 2006, **386**, 427-434.
7 N. Pamme and A. Manz, *Analytical Chemistry*, 2004, **76**, 7250-7256.
8 D. A. Giljohann and C. A. Mirkin, *Nature*, 2009, **462**, 461-464.
9 T. Tachi, N. Kaji, M. Tokeshi and Y. Baba, *Lab on a Chip*, 2009, **9**, 966-971.
10 D. C. Appleyard, S. C. Chapin, R. L. Srinivas and P. S. Doyle, *Nature Protocols*, 2011, **6**, 1761-1774.
11 H. Amini, E. Sollier, M. Masaeli, Y. Xie, B. Ganapathysubramanian, H. A. Stone and D. Di Carlo, *Nat Commun*, 2013, **4**, 1826.
12 D. R. Gossett, H. T. K. Tse, J. S. Dudani, K. Goda, T. A. Woods, S. W. Graves and D. Di Carlo, *Small*, 2012, **8**, 2757-2764.
13 A. P. Tan, J. S. Dudani, A. Arshi, R. J. Lee, H. T. K. Tse, D. R. Gossett and D. Di Carlo, *Lab on a Chip*, 2014.
14 C. Kantak, S. Beyer, L. Yobas, T. Bansal and D. Trau, *Lab on a Chip*, 2011, **11**, 1030-1035.
15 S. E. Chung, W. Park, S. Shin, S. A. Lee and S. Kwon, *Nature Materials*, 2008, **7**, 581-587.
16 R. D. Sochol, S. Li, L. P. Lee and L. Lin, *Lab on a Chip*, 2012, **12**, 4168-4177.
17 R. D. Sochol, M. E. Dueck, S. Li, L. P. Lee and L. Lin, *Lab on a Chip*, 2012, **12**, 5051-5056.

